Received: 14 August 2019 | Revised: 2 March 2020 | Accepted: 9 March 2020

DOI: 10.1002/jbm.a.36924

ORIGINAL ARTICLE

Society For Biomaterials | WILEY

Development of biodegradable membranes for the delivery of a bioactive chitosan-derivative on cartilage defects: A preliminary investigation

Francesca Scognamiglio[1,3] | Andrea Travan[2] | Massimiliano Borgogna[2] | Ivan Donati[1] | Eleonora Marsich[3]

[1]Department of Life Sciences, University of Trieste, Trieste, Italy

[2]Biopolife S.r.l., Trieste, Italy

[3]Department of Medical, Surgical and Health Sciences, University of Trieste, Trieste, Italy

Correspondence
Francesca Scognamiglio, Department of Medical, Surgical and Health Sciences, University of Trieste, Piazza dell'Ospitale 1, 34129 Trieste, Italy.
Email: fscognamiglio@units.it

Funding information
Interreg V-A Italia-Slovenia 2014-2020 bando 1/2016 asse 1, Grant/Award Number: BioApp 1472551605; "Programma Operativo del Fondo Sociale Europeo 2014/2020 della Regione autonoma Friuli Venezia Giulia" (HeAD—Higher Education and Development), Grant/Award Number: FP1619892003

Abstract

Biodegradable membranes for cartilage applications were manufactured starting from polymeric networks of a lactose-modified chitosan (CTL), previously proposed for chondrocytes stimulation. This implantable biomaterial was conceived as a reservoir of a bioactive polymer that could promote the activity of chondrocytes and the healing of cartilage defects. Freeze-drying of reticulated hydrogels enabled to obtain pliable membranes with a homogeneous polymeric texture, as pointed out by scanning electron microscopy analyses. Swelling tests and dimensional evaluations showed that the material is able to absorb physiological fluids and expand gradually upon rehydration. This feature was evaluated on a simulated cartilage defect on pig's humerus (ex vivo), which revealed the capability of the membranes to progressively fit the tissue voids on the damaged cartilage. The rheological properties of the rehydrated membranes pointed out their peculiar strain-stiffening behavior, which represents a promising feature for the regeneration of tissues subjected to variable mechanical loads and deformations. Biological in vitro studies demonstrated the biocompatibility of the membranes in contact with primary chondrocytes and osteoblasts. Taken together, these results represent a starting point for the development of a novel generation of implantable biomaterials for cartilage treatment based on CTL.

KEYWORDS
biodegradable membranes, cartilage, chitosan-derivative, implantable biomaterials, polysaccharides

1 | INTRODUCTION

Articular cartilage is a highly specialized tissue populated by chondrocyte cells that are embedded in an interpenetrated network of collagen fibers (mainly type II) and glycosaminoglycans (GAGs; Armiento, Stoddart, Alini, & Eglin, 2018; Bernhard & Vunjak-Novakovic, 2016). This tissue displays peculiar viscoelastic features and it acts together with the subchondral bone to adsorb and distribute mechanical loads at synovial joints (Pan et al., 2009). Chondrocytes are responsible for the synthesis of a large number of extracellular matrix (ECM) components (collagen, glycoproteins, proteoglycans, and hyaluronan) and for ECM maintenance (Archer & Francis-West, 2003; Sophia Fox, Bedi, & Rodeo, 2009). Some events such as aging, traumas, and the occurrence of inflammatory diseases like osteoarthritis (OA) can affect cartilage structure and functions leading to tissue damages. The repair of cartilage defects poses some challenges due to the limited ability of tissue self-healing and to the fact that current treatments often lead to the synthesis and deposition of

fibrocartilage, which lacks the mechanical and functional properties of hyaline cartilage (Armiento, Alini, & Stoddart, 2019; Karuppal, 2017). The treatment of cartilage damages can be managed by administration of compounds such as corticosteroids (Jüni et al., 2015; Wernecke, Braun, & Dragoo, 2015), hyaluronic acid (Jang et al., 2013; Strauss, Schachter, Frenkel, & Rosen, 2009), and platelet-rich plasma (Altan, Aydin, Erkocak, Senaran, & Ugras, 2014; Montañez-Heredia et al., 2016).

Among the conventional approaches for cartilage regeneration, autologous chondrocyte implantation (ACI), matrix-induced autologous chondrocyte implantation (MACI), or autologous matrix-induced chondrogenesis (AMIC) are the most used (Martín, Patel, Zlotnick, Carey, & Mauck, 2019). In ACI procedures, a section of healthy cartilage is harvested from patients. Chondrocyte cells are isolated from cartilage, expanded in vitro and reimplanted into the defect (Makris, Gomoll, Malizos, Hu, & Athanasiou, 2015). MACI approaches take instead the advantage of using cell-laden scaffolds to be implanted in the defect of cartilage. Indeed, in this procedure chondrocytes are expanded in vitro and seeded into a collagen-based membrane, which will be implanted into the defect site (Dunkin & Lattermann, 2013). Hyaluronic acid can also constitute scaffolds for cell seeding and, as collagen materials, it can stimulate the synthesis of collagen type II and the maintenance of the chondrogenic phenotype (Bian et al., 2011). In AMIC procedures a different approach is followed: the subchondral bone undergoes microfracturing during a surgical intervention, allowing the recruitment of mesenchymal stem cells (MSCs). An acellular scaffold is then implanted at the defect and it is colonized by MSCs to allow the reconstitution of healthy tissue (Benthien & Behrens, 2010). Other approaches involve surgical interventions such as microfractures, a bone marrow stimulating technique, and chondroplasty surgery (Anderson, Rose, Wille, Wiedrick, & Crawford, 2017; Erggelet & Vavken, 2016). A different strategy to promote cartilage regeneration is based on the use of implantable materials which can serve as delivery systems of cells and bioactive molecules (Deng, Chang, & Wu, 2019). As to the materials composition, biomacromolecules such as collagen (Chen, Yao, Wei, & Chu, 2011; Mueller-Rath et al., 2010), hyaluronic acid (Lisignoli et al., 2005; Toh et al., 2010), and chitosan (Hao et al., 2010; Hoemann, Sun, Légaré, McKee, & Buschmann, 2005; Ragetly, Slavik, Cunningham, Schaeffer, & Griffon, 2010) have been used for the treatment of cartilage-related defects. Among these, the scientific interest on chitosan is constantly growing (Pang, Chen, Ji, & Zhong, 2008; Rizwan et al., 2019). One of the main advantages in using chitosan-based biomaterials for cartilage defects treatment deals with its composition, which is similar to that of native cartilage (Duarte Campos, Drescher, Rath, Tingart, & Fischer, 2012). Beside chitosan, also chitosan-derivatives have been employed for cartilage tissue engineering applications (Hsu et al., 2004; Yamane et al., 2005). In this regard, the biological properties of a lactose-modified chitosan (namely "CTL") on chondrocyte cells were explored in vitro by Donati and coworkers. The results of those studies showed that chondrocyte cells cultured on CTL coatings could form cellular aggregates in which an increased synthesis of collagen and GAGs was found with respect to monolayer cell cultures (Donati et al., 2005; Marsich et al., 2008). These results opened for possible applications of this modified polysaccharide in the field of cartilage defect repair. Recent researches on this chitosan-derivative showed that CTL molecules can form dynamic cross-linked polymeric networks in the presence of reticulating agents such as boric acid; these sol/gel systems are endowed with peculiar mechanical properties since they display a strain-hardening behavior upon increasing the stress applied, resembling the features of ECM components like collagen (Cok et al., 2018; Furlani et al., 2019). Based on these premises, this work aims at the development of a CTL-based biomaterial in the form of an implantable membrane that could act as a reservoir of this bioactive polymer in direct contact with articular cartilage, thus opening for potential applications for the treatment of cartilage-related defects.

2 | MATERIALS AND METHODS

2.1 | Materials

Lactose-modified chitosan-hydrochloride form (CTL) with fractions of: N-acetyl-glucosamine (GlcNAc; "acetylated," A) (F_A) = 0.16; glucosamine ($GlcNH_2$; "deacetylated," D) (F_D) = 0.21; lactitol-substituted D unit (N-alkylated GlcLac; "lactitol," L) (F_L) = 0.63 was kindly provided by Biopolife S.r.L. (Trieste, Italy). The intrinsic viscosity [η] determined at 25°C by viscosimetry (CT 1150 Schott Geräte automatic measuring apparatus and a Schott capillary viscometer (Furlani et al., 2019) was found to be 344 ml/g and the estimated molecular weight was 780,000 g/mol. Phosphate-buffered saline (PBS), boric acid (H_3BO_3), sodium chloride, glycerol, triton X-100, hyaluronidase from bovine testes type I-S, collagenase type II, toluidine blue, poly-L-lysine solution, LDH (lactate dehydrogenase)-based TOX-7 kit, formaldheyde, ascorbic acid, ethanol, xylene were all purchased from Sigma Aldrich. Dulbecco modified Eagle medium (DMEM), penicillin/streptomycin and fetal bovine serum (FBS) were purchased from Euroclone S.p.A. For membranes preparation, purified water approved for medical injections (Eurospital) was used.

2.2 | Manufacturing of membranes

CTL membranes reticulated with boric acid were prepared from aqueous solutions of CTL (final concentration of 2% or 3% w/v). Glycerol (final concentration 1% v/v) and PBS 10X (final concentration 1X) were added to the mixture and the pH was set at 7.4. The solution of boric acid (initial concentration 50 m*M*, pH 7.4 in PBS 1X) was added under vigorous mechanical stirring to favor the formation of homogeneous weak hydrogels. The final concentration of boric acid in the mixture was 8 m*M*. Reticulated hydrogels were poured into a mold. In order to get a uniform distribution, 517 μl of hydrogels/cm^2 were employed. The hydrogels were freezed at −20°C overnight and dried under vacuum using a Single-Chamber Freeze-Dryer (Christ Alpha 1-2

LD plus). Two formulations were prepared: CTL 2% w/v, boric acid 8 m*M*, glycerol 1% v/v membrane (short-named C2M) and CTL 3% w/v, boric acid 8 m*M*, glycerol 1% v/v membrane (short-named C3M).

2.3 | Scanning electron microscopy

Membrane samples were positioned on aluminum stubs covered with two-side conductive carbon adhesive tape and gold-sputtered (Sputter Coater K550X, Emitech, Quorum Technologies Ltd., UK). The analysis was performed by means of a Scanning Electron Microscope (Quanta250 SEM, FEI, OR) operated in secondary electron detection mode. The working distance and the accelerating voltage were adjusted in order to obtain a suitable magnification.

2.4 | Swelling test

The swelling behavior of C2M and C3M was investigated in phosphate buffer solution (PBS 1X). Membrane samples of circular shape (d = 20 mm) were weighted and immersed in PBS 1X solution. At each selected time points the membranes were collected, the excess of solution was removed by drying the samples on a paper for 30 s and the weight of the wet membranes was measured. A total of 8 ml of PBS was added stepwise in each well containing the membrane. The swelling ratio (s.r.) was calculated according to Equation (1).

$$\text{s.r.}(\%) = (Ws - Wd)/Wd*100 \quad (1)$$

where Ws and Wd are the weight of swollen and dry membranes, respectively. Five replicates were considered for the analyses.

2.5 | Degradation tests

Membrane samples (1 cm × 1 cm) were immersed in PBS 1X solution (2 ml) and incubated at 37°C. Once per day, the membranes were collected, the excess of water removed by drying on filter papers for 30 s and their weight recorded. PBS 1X (2 ml) was added after 1 and 2 days. As reference, the 100% of the weight was considered as the weight of the samples after 2 hr of immersion in PBS 1X. Three parallel replicates were considered for this study.

2.6 | Evaluation of the lateral expansion of membranes

The dimensional expansion of the membranes occurring upon rehydration was evaluated by measuring the radial expansion of the samples immersed in phosphate buffer solution (PBS 1X) over time. Circular shaped membranes (d = 11 mm) were placed on the wells of a 24-well plate and PBS 1X solution was added to the wells (2 ml). Pictures of the samples were acquired at selected time points, maintaining a fixed distance between the samples and the camera's lens (9 cm). The pictures were analyzed with a software for image analyses (ImageJ): the membrane area was outlined and the percentage of size expansion (s.e.) was calculated as a function of time according to Equation (2):

$$\text{s.e.}(\%) = (Ss - Sd)/Sd*100 \quad (2)$$

where Ss was the size of the swollen membrane at each time point considered and Sd was the size of the dry membrane, respectively. Given the small thickness of the membranes, thickness variations were considered negligible. Three replicates were considered for this test.

2.7 | Hands-on ex vivo evaluation of membrane on cartilage defect

A cartilage defect (d = 10 mm) was performed on articular cartilage of freshly harvested humerus from adult pig provided by a slaughterhouse. The subchondral bone was exposed and C2M samples of circular shape (d = 7.5 mm) were applied on the defect. The membranes were rehydrated with water for injection (1 ml) and photographs of membrane were acquired 1 and 5 min after hydration to monitor radial expansion of membrane. After 1 and 3 min from rehydration, an additional volume of water (1 ml) was added to wet membranes.

2.8 | Rheological analyses on rehydrated membranes

Long stress-sweep measurements on CTL-boric acid hydrogels and rehydrated membranes were performed by means of a controlled stress rheometer Haake Rheo-Stress RS150 operating at 37°C, using a roughened plate device (HPP20 profiliert: Ø = 20 mm; frequency: 1 Hz; gap: 0.4 mm). Membrane samples (0.8 cm × 0.8 cm) were immersed in PBS 1X (0.5 ml) and incubated at 37°C for 24 hr to allow liquid uptake. After incubation, the rehydrated membranes were collected and employed for the measurements. During each measurement, a solvent trap was used to prevent sample evaporation.

2.9 | Isolation of porcine articular chondrocytes

Chondrocyte cells were isolated from thin slices of knee-articular cartilage from adult pigs provided by a slaughterhouse. Starting from cartilage tissue slices, chondrocytes were isolated by an enzymatic digestion of tissues according to a procedure previously described (Grandolfo et al., 1993). Briefly, thin slices of tissue were obtained from articular cartilage and incubated with a solution containing hyaluronidase (270 U/ml), penicillin (500 U/ml) and streptomycin (500 U/ml) for enzymatic digestion. Incubation was carried out at

37°C for 1 hr. Tissue slices were then collected and incubated with collagenase type II (250 U/ml), penicillin (500 U/ml), streptomycin (500 U/ml) under vigorous shaking, at 37°C overnight. Remnants of tissue fragments were removed by filtration from the solution and isolated cells were cultured in DMEM supplemented with 10% FBS, 0.25% penicillin/streptomycin, at 37°C and 5% pCO_2.

2.10 | In vitro biocompatibility (LDH assay)

LDH assay was employed to assess the biocompatibility of CTL membranes on osteoblasts (Osteosarcoma MG-63 cell line, ATCC number: CRL-1427) and primary chondrocytes. Cells were cultured in DMEM supplemented with 10% FBS and 0.25% penicillin/streptomycin, at 37°C and 5% pCO_2. Cells were plated on a 24-well plate at the final density of 50,000 cell/well. The day after seeding, membrane samples (d = 6 mm) were UV-sterilized and added to the wells. Cells cultured in plain medium and treated with Triton X-100 0.01% in DMEM were employed as negative and positive control of cell death, respectively. The LDH assay was performed 24 and 72 hr after treatment. The level of cytotoxicity was evaluated considering the total amount of intracellular LDH, obtained by treating cells with a lysis-inducing solution. For the assay, cellular medium from each sample (45 μl) was incubated with the LDH mix solution (30 μl LDH assay substrate, 30 μl LDH cofactor, 30 μl dye solution) for 30 min in dark. The enzymatic reaction was stopped by adding 1/10 volume of HCl 1 N to each well. The plate was read at 490 nm and 690 nm with a spectrophotometer (Infinite M200PRO NanoQuant, Tecan). For each sample, the percentage of LDH release was calculated by normalizing the absorbance values of treated or control (untreated) cells to the absorbance of the cellular lysis, at each time point considered. For each series of samples, four replicates were considered.

2.11 | Preparation of membrane extracts

CTL membranes used for the treatment of chondrocytes for the analyses of cellular morphology were prepared according to the procedure described above (Section 2.2), without the addition of glycerol to the mixture. Indeed, the presence of glycerol in membrane extract might prevent the staining of cells with toluidine blue. To prepare membrane extracts, membrane samples (150 mg) were UV-sterilized and incubated in DMEM (30 ml) for 72 hr at 37°C. The ratio between medium volume and weight of membrane was calculated in order to reach a maximum CTL concentration of 0.5%.

2.12 | Qualitative evaluation of cell morphology by toluidine blue staining

To promote cellular adhesion, glass coverslip (Zeus Super; d = 13 mm) were coated by incubation with a poly-L-lysine solution (final concentration 0.01% w/V). After 1 hr, the excess of solution was removed, glasses were washed with water for injection and UV-sterilized. Chondrocyte cells were seeded on glass coverslips at the final density of 50,000 cells/coverslip. The day after seeding, cells were treated with membrane extracts or with plain medium in the case of control (final volume = 1 ml). Ascorbic acid was then added to each well (final concentration 100 nm). After 4 and 7 days from treatment, cellular medium was removed, cells were washed with PBS 1X and fixed with formaldehyde 4X in PBS 1X for 30 min. Cells were washed with deionized water and gradually dehydrated in ethanol (30%, 50%, 70%, 95%, and 100%), each step for 10 min. After dehydration, cells were treated with xylene and dried. Glasses were mounted with Leica-CV mountant on microscope slides (Materglass 26 × 76 mm—1.0/1.2 mm thick). Images of samples were acquired with a Zeiss Axiophot microscope.

3 | RESULTS

3.1 | Manufacturing of membranes and morphological analyses

Membranes based on CTL were prepared starting from a cross-linked polymeric network of CTL chains reticulated with boric acid. As a plasticizer, glycerol was added to the CTL-mixture. The addition of boric acid to the polysaccharide mixture enables the formation of a cross-linked polymeric network as reported in Furlani et al. (2019). To explore the possibility to employ different amounts of CTL within the membranes (keeping constant the amounts of cross-linker and plasticizer), two compositions were considered starting from hydrogels with 2% w/V or 3% w/V of CTL, in order to obtain the resulting membranes (respectively "C2M" or "C3M" as detailed in Section 2). After freeze-drying the reticulated hydrogels, soft and pliable membranes with a homogeneous texture where obtained, as shown in Figure 1.

Scanning electron microscopy (SEM) allowed to investigate more in the detail the morphological features of the membranes and to evaluate the homogeneity of membrane surface and their porosity. The analyses pointed out the homogeneous textures of membranes (Figure 2a,c). Cross-section images of both membranes showed the presence of pores throughout the membrane thickness (Figure 2b,d); membrane porosity might facilitate their rehydration by absorption of fluids, after placement at the synovial joints.

The C3M displays a more compact structure than C2M, which can be ascribed to the presence of higher polymer content. The images pointed out that the thickness of the membranes is in the range of 1 ÷ 2 mm, depending on the composition (amount of polymer).

3.2 | Swelling tests and lateral expansion of membranes

The swelling behavior and the lateral expansion of the membranes in liquid environment was investigated in PBS solution to predict their

FIGURE 1 C2M membranes (upper row) and C3M membranes (lower row) reticulated with boric acid. The CTL-membrane displays a homogeneous texture and pliability. CTL, lactose-modified chitosan

ability to absorb surrounding fluids and to fill cartilage defect upon positioning at the implant site. The samples were incubated in PBS and, at selected time points, the membranes (C2M and C3M) were collected, the excess of water removed, and the weight of rehydrated membranes was recorded. The swelling profile of membranes pointed out a remarkable increase of the swelling ratio few minutes after soaking, an ability that can be ascribed to their hydrophilic feature and porous structure. After a step of fast and massive swelling within the first 30 min, the process of liquid uptake occurs more slowly and gradually over time and it reaches a plateau after 2 hr of incubation (Figure 3a).

When rehydrated, the membranes could also increase their size by radial expansion. The extent of such size increase with respect to the size of dry membranes was evaluated over time (Figure 3b).

The results pointed out that already few minutes after rehydration, the membrane could radially increase their size up to 16% and 25% of their initial dimensions, for C3M and C2M, respectively. No significant additional increase of radial expansion was noticed with prolonged incubation time (Figure 3b).

The ability of these membranes to expand upon rehydration represents an additional advantage, since they can act as "self-fitting" materials that expand in contact with physiological fluids and tend to adapt to the implant site (in this case cartilage defects). To further describe this behavior, a qualitative ex vivo evaluation was carried out by creating a cartilage defect on pig's humerus; then, the membrane was placed within the defect site, rehydrated with 1 ml of water in order to evaluate the size expansion as a function of time (Figure 4).

After rehydrating the CTL-based membrane (C2M) within the defect site, the material was able to enlarge radially and adapt to the cartilage-devoid area, thus forming a continuous layer with the surrounding cartilage. After few minutes, the gradual expansion of the membrane led to a complete filling of the cartilage defect (Figure 4). Similar results were obtained when C3M samples were employed (data not shown).

3.3 | Rheological analyses on hydrogels and rehydrated membranes

The rheological properties of CTL-boric acid hydrogels and rehydrated membranes were investigated by long stress-sweep measurements, considering composition with CTL 2% w/v (Figure 5a) and CTL 3% w/v (Figure 5b).

These analyses enabled to evaluate the variation of the elastic (G') and loss (G'') moduli as a function of the applied stress (τ) and to investigate whether the manufacturing procedures (freeze-drying) affects the rheological properties of membranes after rehydration

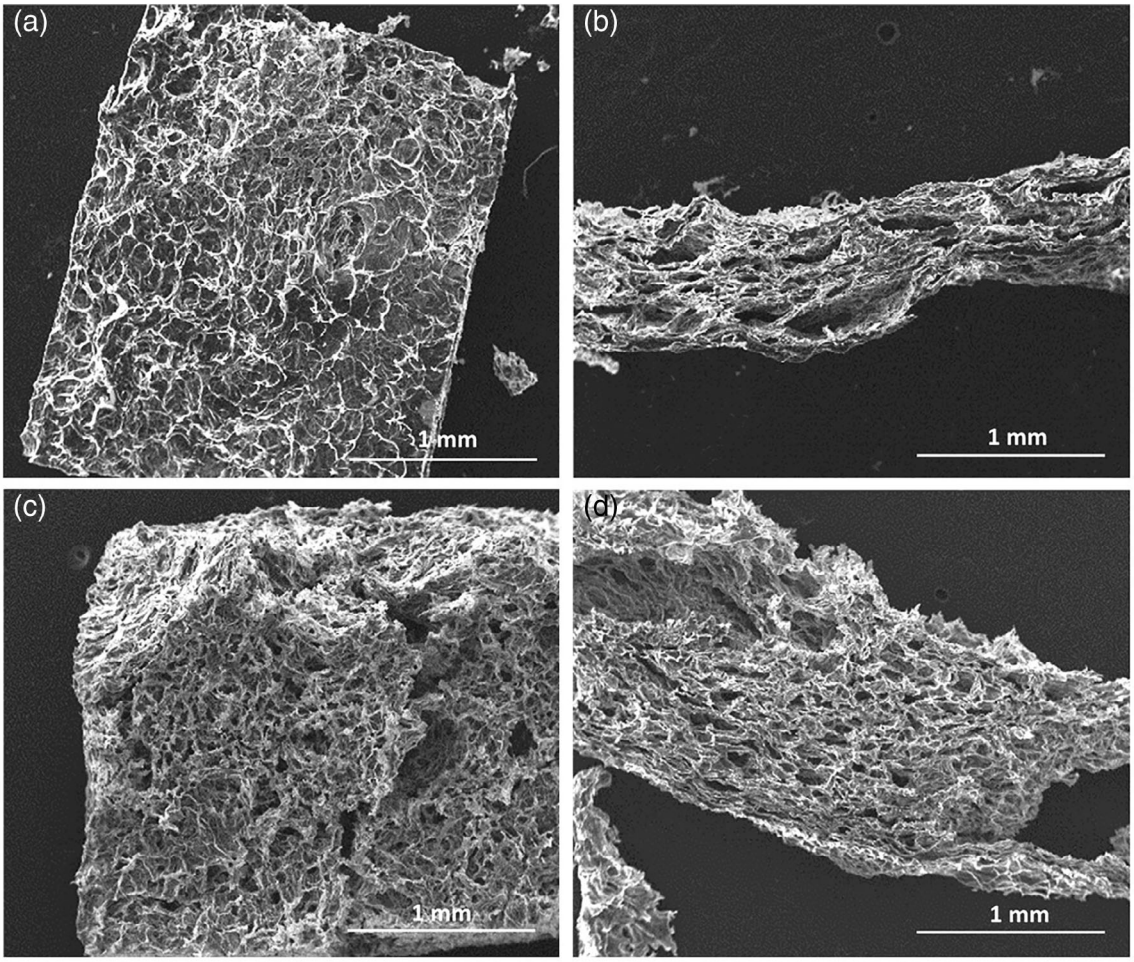

FIGURE 2 SEM images of C2M (a: top view; b: cross section) and C3M (c: top view; d: cross section). SEM, scanning electron microscopy

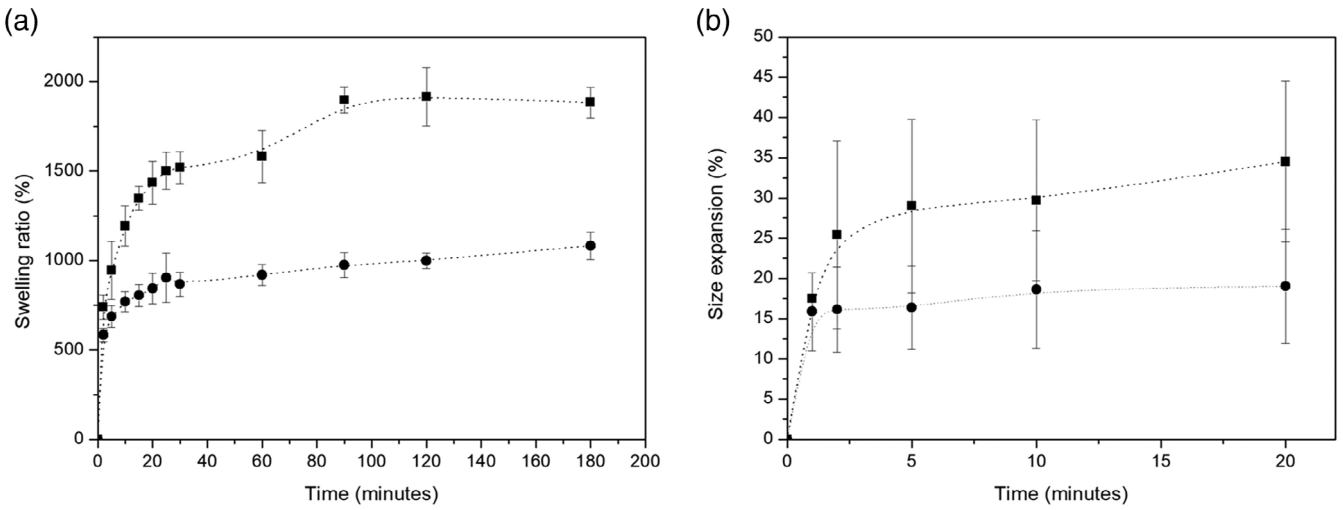

FIGURE 3 Swelling kinetics (a) and radial expansion behavior (b) on C2M (squares) and C3M (rounds). Dashed lines are drawn to guide the eye

(i.e., after implantation). The data pointed out that both hydrogels and rehydrated membranes display a strain-hardening behavior, which is typical of CTL-boric acid systems (Cok et al., 2018; Furlani et al., 2019). Interestingly, this feature is retained after the freeze-drying process, indicating that the manufacturing procedure did not alter the peculiar mechanical behavior of the CTL-boric acid systems.

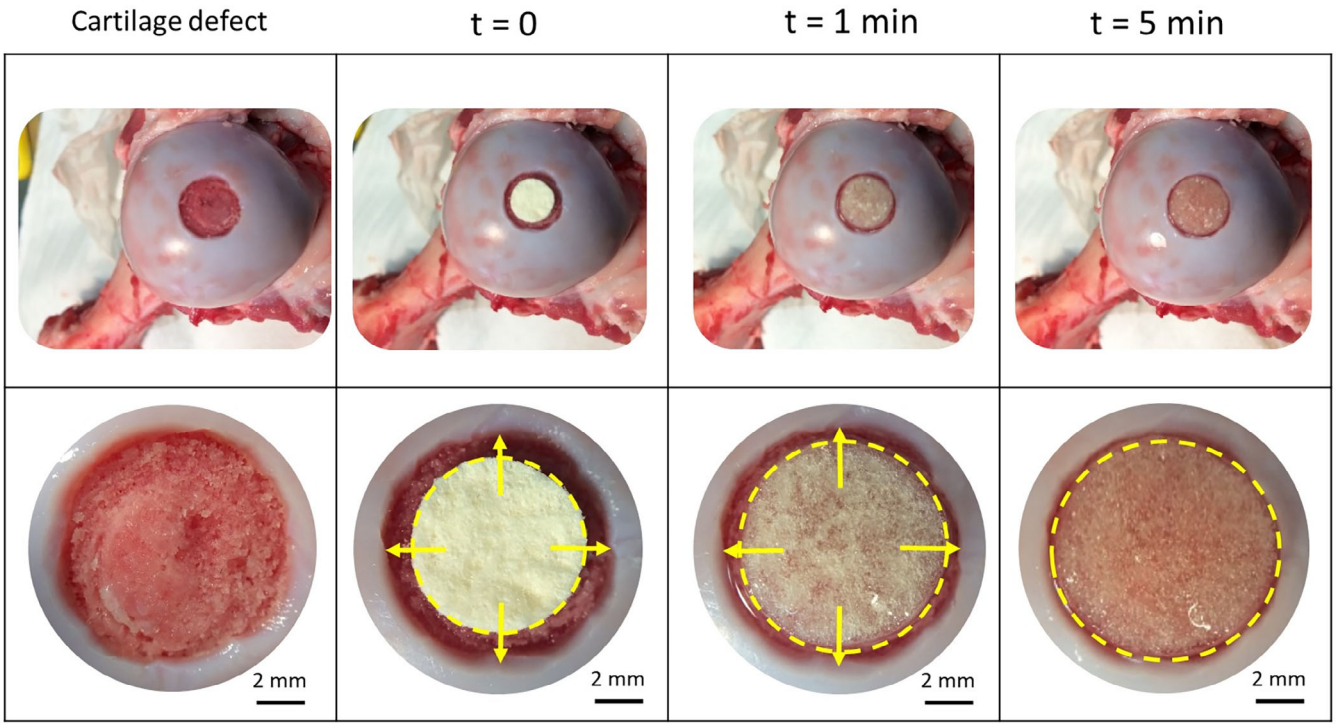

FIGURE 4 Simulation of implantation of a CTL-based membrane (C2M) within a cartilage defect: ex vivo evaluation of membrane expansion upon rehydration with water. The lower row shows a ×10 zoom of the upper row. Dashed lines indicates membrane size. Arrows are drawn to highlight the process of radial expansion

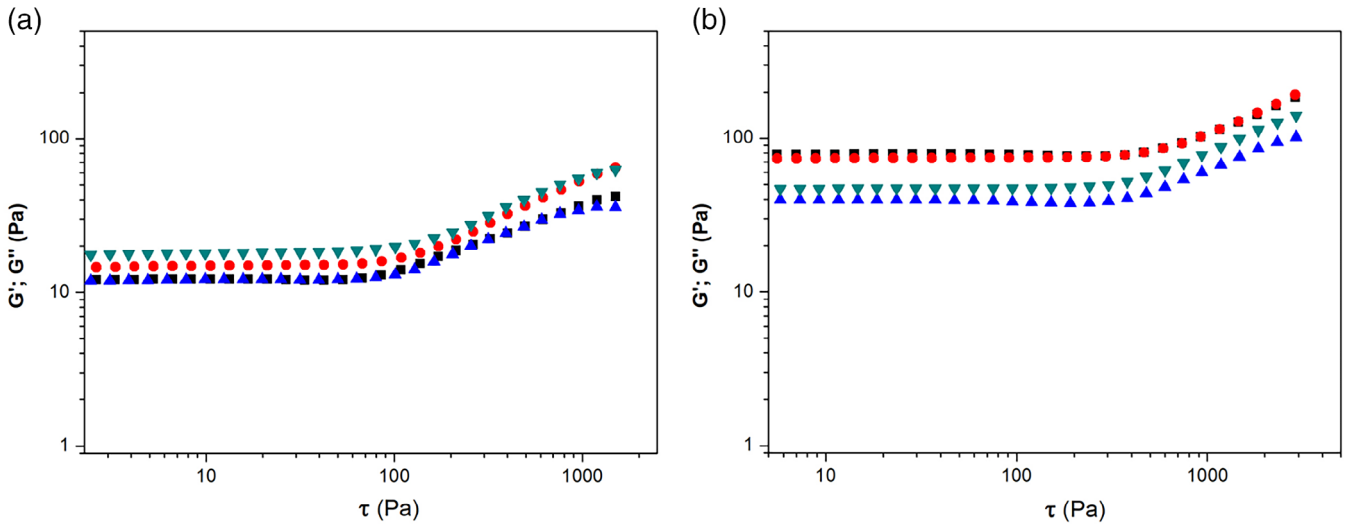

FIGURE 5 Long stress-sweep measurements on hydrogels and rehydrated C2M and C3M. The compositions with different CTL concentration—CTL 2% (a) and CTL 3% (b)—were considered (black squares: G' of membranes; red rounds: G'' of membranes; blue triangles: G' hydrogels, green triangles: G'' hydrogels). CTL, lactose-modified chitosan

3.4 | Degradation of membranes

Degradation studies were performed in PBS solution to predict the degradation kinetics of the membranes after implantation (Figure 6). It is expected that, when in contact with biological fluids, CTL membranes undergo a progressive degradation due to the dissociation of boric acid. Indeed, the reticulation given by boric acid does not involve covalent interactions, but rather transient ones where boric acid is in equilibrium between the bound and unbound state (Cok et al., 2018).

Figure 6 shows that the membranes are gradually degraded in physiological environment and that the process lasts for about 48 hr. No influence of degradation kinetics from membrane composition

was observed. This result suggests that already during the first hours after the contact with fluids, increasing amounts of CTL solubilize thus becoming rapidly available to the surrounding tissue.

3.5 | In vitro biocompatibility (LDH assay)

To investigate the biocompatibility of membranes in vitro, LDH assay was performed on an osteoblast cell line (MG-63) and on primary chondrocytes extracted from pig's articular cartilage. This study was performed by means of LDH assay, associated to a morphological evaluation of cell morphology by toluidine blue staining. The results showed that for both cell types there were no considerable differences in terms of LDH released, considering cells cultured in contact with membranes (C2M and C3M) and the negative control (untreated cells). On the contrary, in the case of cells treated with Triton X-100 (positive control of cell toxicity) the percentage of LDH enzyme released in cellular medium was increased (Figure 7a,b). A visual evaluation of both cell types confirmed the LDH results, pointing out the healthy morphology retained by cells in the presence of the membranes.

A qualitative evaluation of membrane biocompatibility on chondrocytes was carried out with optical microscope. Cells were grown in adhesion in the presence of C2M or C3M extracts and, at selected time points, cells were stained with toluidine blue to highlight cellular morphology (Figure 8). It can be noticed that the morphology of cells treated with membrane extracts was comparable to that of untreated cells, both 4 and 7 days after treatment.

Both in the case of treated cells and control samples, the cells appear well adherent, flatted and spread on the substrate, and display a polygonal shape typical for chondrocytes grown on 2D systems. The nucleus and nucleolus have well defined edges, and in the cytoplasm are not visible lacunae or vacuoles. Cell–cell interactions are evident at day 4 from seeding but extended cytoplasm cell–cell processes appear more pronounced at day 7 of culture.

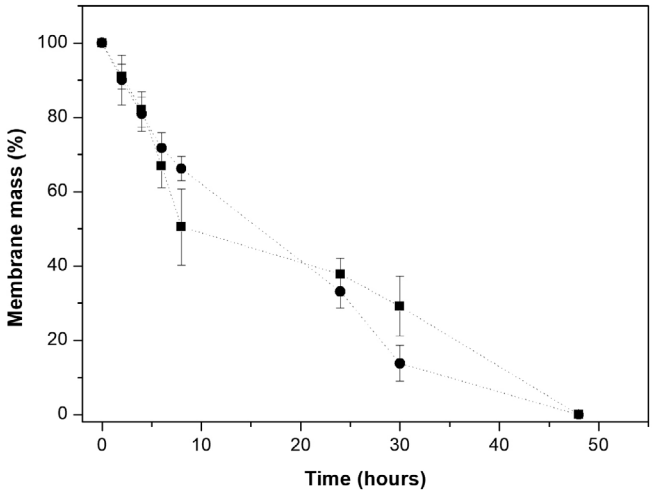

FIGURE 6 Degradation kinetics of C2M (squares) and C3M (rounds)

3.6 | Discussion

Cartilage tissue undergoes modifications of its structure and function upon the occurrence of injuries, inflammatory diseases or aging. Whether one of these events occurs, tissue integrity can be compromised, leading to cartilage damage. To prevent the consequences of such event, novel biomaterials capable of limiting structural damages and contributing to the maintenance of tissue functionality are continuously sought (Jeuken et al., 2016; Sánchez-Téllez, Téllez-Jurado, & Rodríguez-Lorenzo, 2017). One of the main mechanisms contributing to the loss of cartilage integrity and functionality reported in the case of traumas or OA deals with the degradation of

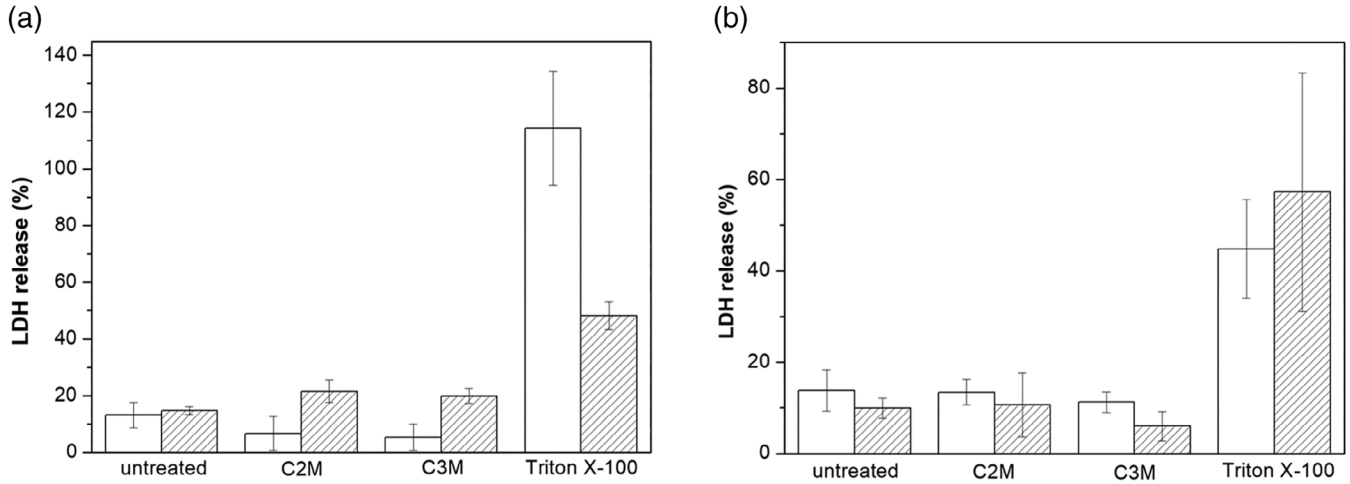

FIGURE 7 In vitro biocompatibility (LDH assay) on osteoblasts (a) and chondrocytes (b) treated with CTL-boric acid membranes at 24 hr (white bars) and 72 hr (patterned bars) from treatment. LDH, lactate dehydrogenase

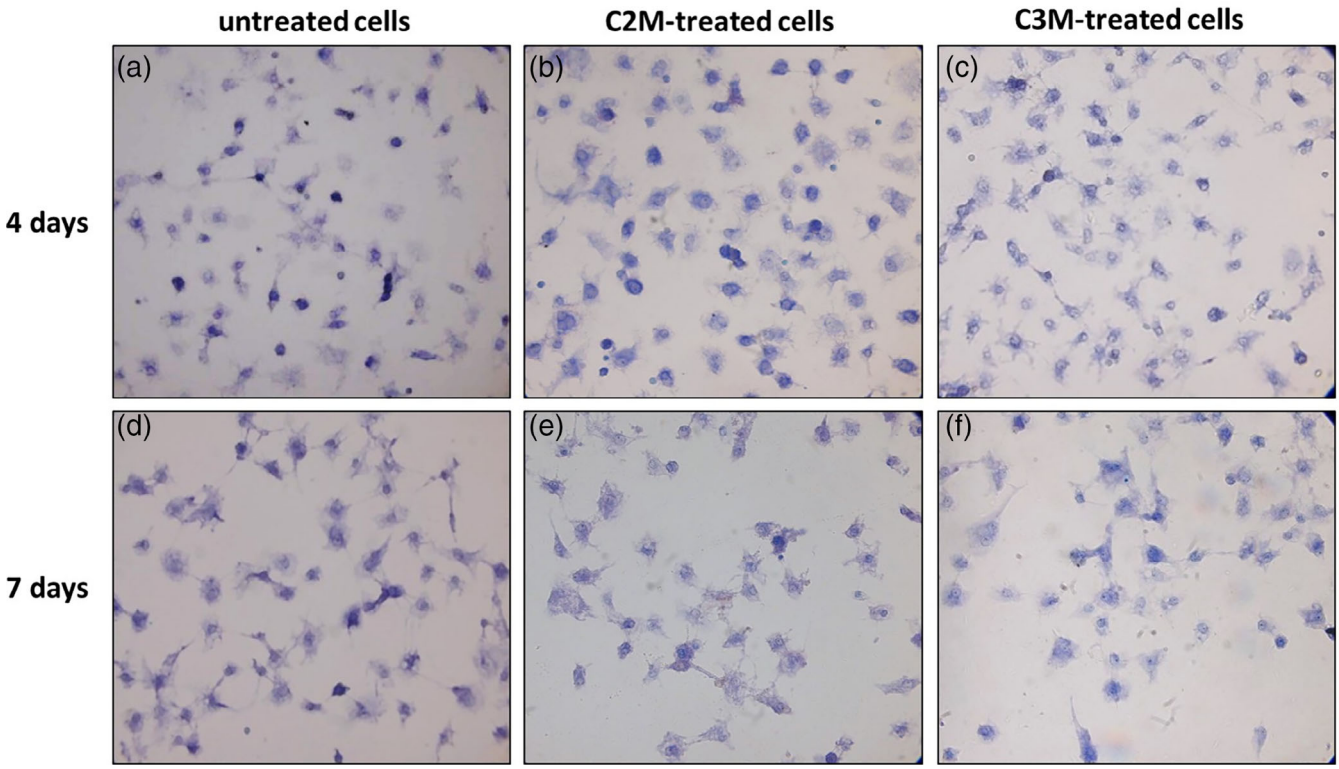

FIGURE 8 Optical images (×40) of chondrocytes stained with toluidine blue. Upper row: untreated cells (a), cells treated with C2M extracts (b), and C3M extracts (c) 4 days after treatment. Lower row: untreated cells (d), cells treated with C2M extracts (e), and C3M extracts (f) 7 days after treatment

collagen (Poole et al., 2002). The bioactive response induced in vitro by the polymer CTL in terms of enhancing the synthesis of collagen and GAGs in chondrocyte aggregates (Donati et al., 2005; Marsich et al., 2008) makes this modified polysaccharide an appealing choice to limit cartilage damage and favor the recovery of tissue functionality. A recent paper by Salamanna et al. (2019) evaluated preclinical therapeutic effects of intra-articular injections of a formulation of CTL in mixture with hyaluronic acid (HA) on OA rat models; this study showed that the CTL-based formulation caused a significant improvement in the treatment of knee-articular cartilage degeneration and synovium inflammation as compared to HA-treated and nontreated animals. Given these premises, materials based on CTL can be exploited as tools to deliver efficiently the bioactive polysaccharide at synovial site. The CTL-based membranes developed in this work were designed to act as a resorbable local reservoir of CTL, potentially enabling the release of high local concentration of this polysaccharide within few hours from application. Moreover they were devised to be pliable (for ease of surgical implantation), adaptable to the shape of cartilage defects and readily prone to rehydration in contact with biological fluids. The process of membrane manufacturing (hydrogel preparation followed by freeze-drying) enabled the preparation of membranes with a smooth surface and homogeneous structure (Figure 1). SEM analyses highlighted the porous structure of the freeze-dried membranes (Figure 2), which is a desired feature in order to favor the process of liquids uptake. In fact, the results obtained by swelling tests pointed out that, when immersed in PBS, the membranes rapidly swell and adsorb considerable liquid amounts immediately after soaking (Figure 3a). These results are in line with recent research studies stressing the importance of the porosity of polymeric scaffolding materials for cartilage repair applications and pointing out the importance of porous materials to guide the regeneration of a functional tissue (Browe et al., 2019; Nava, Draghi, Giordano, & Pietrabissa, 2016; Song et al., 2017). One of the advantages of the proposed system is that membranes formulation can be tailored to deliver variable amounts of the bioactive polysaccharide CTL at the lesioned site. Moreover, it can be hyphothesized a single-step surgical procedure for the implantation of the membranes at the target site, which would reduce time of intervention and clinical drawbacks. In fact, this explorative study demonstrates that both low (2% in the C2M membranes) and high (3% in the C3M membranes) amounts of CTL within the formulation can be employed to obtain membranes with the desired range of properties. The two membrane compositions tested display different swelling kinetics: the C2M membrane shows a higher swelling than the C3M membrane in the first hours after rehydration. As expected, the swelling profile seems to be influenced by membrane composition and, in particular, by the polymer-crosslinker ratio. Indeed, the C2M displays a higher swelling ability than C3M; this feature can be ascribed to the fact that in the presence of lower amount of polymer, there are less cross-linking points inside the polymeric network, which decreases the compactness of the membrane and favors the

process of liquid uptake. Upon increasing the amount of CTL, the equilibrium between bound and unbound state of boric acid is shifted toward the former, increasing the overall number of cross-links, and thus the compactness of the structure. This is also evident from the higher G′ values obtained for the stress-sweep measurements in the case of C3M and corresponding hydrogels with respect to CTL 2% formulation. In line with these results, it has been recently reported that the swelling behavior of scaffolding materials for cartilage applications is influenced by the cross-linking degree of polymer-composing scaffolds (Song et al., 2017) and by material composition (Liao, Qu, Chu, Zhang, & Qian, 2015). During the swelling of the CTL-based membranes, a dimensional increase can be observed from the first minutes (Figure 3b); the evaluation of the expansion upon hydration pointed out that, already during the first 20 min, an increase of membranes size in the range of 19–34% occurred (Figure 3b). The extent of such increase is influenced by membrane composition: C2M displays a more pronounced size variation than the C3M membrane, which parallels the swelling behavior. The qualitative evaluation performed on a simulated cartilage defect confirmed this feature (Figure 4); in fact, once wet, the material is able to adapt to the defect shape and fit defect voids by a progressive lateral expansion.

The hydrophilic feature of the CTL-based membranes and the ability to rehydrate in the presence of liquids represents an additional desired feature for the treatment of cartilage damages characterized by a reduced tissue hydration. Indeed, a reduction of matrix hydration (occurring for instance during aging) has been related to an undesired variation of its compressive stiffness (Akkiraju & Nohe, 2015). In this view, the use of a biomaterial that can contribute to the maintenance of a moist environment in the damaged site might provide an additional advantage to preserve cartilage functionality.

After the initial swelling, the degradation studies showed that both CTL-based membranes start to degrade in a comparable manner for about 48 hr, which enables to deliver effectively the bioactive polysaccharide from the early stage of tissue healing. The process of liquid uptake favors the physical transition of membranes to a gel-like state. Considering the nonlinear mechanical behavior of the CTL-boric acid aqueous systems when subjected to mechanical stresses (Cok et al., 2018), the rheological properties of the rehydrated membranes and of the native hydrogels were studied. Rheological measurements on the CTL-boric acid native hydrogels showed a nonlinear response of these systems on applied stress (stress-stiffening behavior). This aspect has already been reported on similar CTL-based systems and it can be traced back to the transient nature of the borate reticulations (Cok et al., 2018). It can also be noticed that the hydrogels containing a higher amount of CTL (3%) display an approximatively 4-times higher elastic modulus than the hydrogel with 2% CTL. As to the membranes, the freeze-drying process required for membranes preparation inevitably alters the structure of the constructs, introducing a porous structure. However, it is noteworthy that the rehydrated samples still maintain the stress-stiffening features, which may represent an innovative feature for biomaterials implanted at cartilage during the first stage of tissue healing. Interestingly, the rheological measurements show that there is basically no loss of mechanical performance upon freeze-drying for both membrane types. This peculiar behavior might represent an advantage to preserve cartilage functionality, since it allows the distribution of mechanical loads between junctions, which contributes to the maintenance of tissue functionality.

In vitro biological tests demonstrated the biocompatibility of the membranes on both primary chondrocytes and on an osteoblasts cell line (Figure 7a,b). The LDH data indicate that the treatment of both cell types with membrane extracts did not alter cellular viability. These results are supported by qualitative analyses on the morphology of chondrocytes in direct contact with membranes extracts over 7 days; in fact, the chondrocytes stained with toluidine blue, showed that the cells treated with membrane extracts retain a morphology comparable to that of control cells until 7 days after treatment (Figure 8a–f).

4 | CONCLUSIONS

This preliminary study paves a way toward the employment of an emerging bioactive polysaccharide (CTL) in a physical form (membrane) specifically devised for the treatment of cartilage defects/damages and which might be implanted at the target site by one-step surgical procedure. On the physical side, the most intriguing features of these membranes include the capability of adapting to cartilage defects and of displaying a stress-hardening behavior, before being completely degraded/solubilized by biological fluids. Moreover, in light of the biocompatibility and of the renown biological activity of this polysaccharide, it can be hypothesized that CTL molecules released at the synovial space could promote chondrocyte activity for instance in terms of matrix synthesis stimulation, which is fundamental in cartilage repair and maintenance. Further in vitro/in vivo studies are necessary to confirm the biological potential of these new constructs. Taken together, these promising results represent a starting point for the development of a novel generation of implantable biomaterials for cartilage defects treatment.

ACKNOWLEDGMENTS

The authors acknowledge Dr. Davide Porrelli for technical support in SEM analyses, and Ms. Chiara Pizzolitto for technical aid in biological tests. This study was supported by Regione Autonoma Friuli Venezia Giulia - Progetto HEaD "Higher Education and Development" Units Operazione 2 - (Codice FP1619892003, canale di finanziamento 1420AFPLO2) - Fondo Sociale Europeo - Investimenti in favore della crescita e dell'occupazione - POR 2014-2020 and by Interreg V-A Italia-Slovenia 2014-2020 bando 1/2016 asse 1—project BioApp 1472551605.

CONFLICT OF INTEREST

The authors declare no potential conflict of interests.

REFERENCES

Akkiraju, H., & Nohe, A. (2015). Role of chondrocytes in cartilage formation, progression of osteoarthritis and cartilage regeneration. *Journal of Developmental Biology*, *3*, 177–192.

Altan, E., Aydin, K., Erkocak, O., Senaran, H., & Ugras, S. (2014). The effect of platelet-rich plasma on osteochondral defects treated with mosaicplasty. *International Orthopaedics*, *38*, 1321–1328.

Anderson, D. E., Rose, M. B., Wille, A. J., Wiedrick, J., & Crawford, D. C. (2017). Arthroscopic mechanical chondroplasty of the knee is beneficial for treatment of focal cartilage lesions in the absence of concurrent pathology. *Orthopaedic Journal of Sports Medicine*, *5*, 2325967117707213.

Archer, C. W., & Francis-West, P. (2003). The chondrocyte. *The International Journal of Biochemistry & Cell Biology*, *35*, 401–404.

Armiento, A. R., Alini, M., & Stoddart, M. J. (2019). Articular fibrocartilage—Why does hyaline cartilage fail to repair? *Advanced Drug Delivery Reviews*, *146*, 289–305.

Armiento, A. R., Stoddart, M. J., Alini, M., & Eglin, D. (2018). Biomaterials for articular cartilage tissue engineering: Learning from biology. *Acta Biomaterialia*, *65*, 1–20.

Benthien, J. P., & Behrens, P. (2010). Autologous matrix-induced Chondrogenesis (AMIC): Combining microfracturing and a collagen I/III matrix for articular cartilage resurfacing. *Cartilage*, *1*, 65–68.

Bernhard, J. C., & Vunjak-Novakovic, G. (2016). Should we use cells, biomaterials, or tissue engineering for cartilage regeneration? *Stem Cell Research & Therapy*, *7*, 56.

Bian, L., Zhai, D. Y., Tous, E., Rai, R., Mauck, R. L., & Burdick, J. A. (2011). Enhanced MSC chondrogenesis following delivery of TGF-β3 from alginate microspheres within hyaluronic acid hydrogels in vitro and in vivo. *Biomaterials*, *32*, 6425–6434.

Browe, D. C., Mahon, O. R., Díaz-Payno, P. J., Cassidy, N., Dudurych, I., Dunne, A., … Kelly, D. J. (2019). Glyoxal cross-linking of solubilized extracellular matrix to produce highly porous, elastic, and chondropermissive scaffolds for orthopedic tissue engineering. *Journal of Biomedical Materials Research*, *107*, 2222–2234.

Chen, W. C., Yao, C. L., Wei, Y. H., & Chu, I. M. (2011). Evaluating osteochondral defect repair potential of autologous rabbit bone marrow cells on type II collagen scaffold. *Cytotechnology*, *63*, 13–23.

Cok, M., Sacco, P., Porrelli, D., Travan, A., Borgogna, M., Marsich, E., … Donati, I. (2018). Mimicking mechanical response of natural tissues. Strain hardening induced by transient reticulation in lactose-modified chitosan (chitlac). *International Journal of Biological Macromolecules*, *106*, 656–660.

Deng, C., Chang, J., & Wu, C. (2019). Bioactive scaffolds for osteochondral regeneration. *Journal of Orthopaedic Translation*, *17*, 15–25.

Donati, I., Stredanska, S., Silvestrini, G., Vetere, A., Marcon, P., Marsich, E., … Vittur, F. (2005). The aggregation of pig articular chondrocyte and synthesis of extracellular matrix by a lactose-modified chitosan. *Biomaterials*, *26*, 987–998.

Duarte Campos, D. F., Drescher, W., Rath, B., Tingart, M., & Fischer, H. (2012). Supporting biomaterials for articular cartilage repair. *Cartilage*, *3*, 205–221.

Dunkin, B. S., & Lattermann, C. (2013). New and emerging techniques in cartilage repair: MACI. *Operative Techniques in Sports Medicine*, *21*, 100–107.

Erggelet, C., & Vavken, P. (2016). Microfracture for the treatment of cartilage defects in the knee joint—A golden standard? *Journal of Clinical Orthopaedics and Trauma*, *7*, 145–152.

Furlani, F., Sacco, P., Scognamiglio, F., Asaro, F., Travan, A., Borgogna, M., … Donati, I. (2019). Nucleation, reorganization and disassembly of an active network from lactose-modified chitosan mimicking biological matrices. *Carbohydrate Polymers*, *208*, 451–456.

Grandolfo, M., D'Andrea, P., Paoletti, S., Martina, M., Silvestrini, G., Bonucci, E., & Vittur, F. (1993). Culture and differentiation of chondrocytes entrapped in alginate gels. *Calcified Tissue International*, *52*, 42–48.

Hao, T., Wen, N., Cao, J. K., Wang, H. B., Lü, S. H., Liu, T., … Wang, C. Y. (2010). The support of matrix accumulation and the promotion of sheep articular cartilage defects repair in vivo by chitosan hydrogels. *Osteoarthritis and Cartilage*, *18*, 257–265.

Hoemann, C. D., Sun, J., Légaré, A., McKee, M. D., & Buschmann, M. D. (2005). Tissue engineering of cartilage using an injectable and adhesive chitosan-based cell-delivery vehicle. *Osteoarthritis and Cartilage*, *13*, 318–329.

Hsu, S., Whu, S. W., Hsieh, S. C., Tsai, C. L., Chen, D. C., & Tan, T. S. (2004). Evaluation of chitosan-alginate-hyaluronate complexes modified by an RGD-containing protein as tissue-engineering scaffolds for cartilage regeneration. *Artificial Organs*, *28*, 693–703.

Jang, J. D., Moon, Y. S., Kim, Y. S., Choi, N. Y., Mok, H. S., Kim, Y. J., … Kim, S. J. (2013). Novel repair technique for articular cartilage defect using a fibrin and hyaluronic acid mixture. *Journal of Tissue Engineering and Regenerative Medicine*, *10*, 1–9.

Jeuken, R. M., Roth, A. K., Peters, R. J. R. W., Van Donkelaar, C. C., Thies, J. C., Van Rhijn, L. W., & Emans, P. J. (2016). Polymers in cartilage defect repair of the knee: Current status and future prospects. *Polymers (Basel)*, *8*, 219.

Jüni, P., Hari, R., Rutjes, A. W., Fischer, R., Silletta, M. G., Reichenbach, S., & da Costa, B. R. (2015). Intra-articular corticosteroid for knee osteoarthritis. *Cochrane Database of Systematic Reviews*, CD005328.

Karuppal, R. (2017). Current concepts in the articular cartilage repair and regeneration. *Journal of Orthopaedics*, *14*, A1–A3.

Liao, J., Qu, Y., Chu, B., Zhang, X., & Qian, Z. (2015). Biodegradable CSMA/PECA/graphene porous hybrid scaffold for cartilage tissue engineering. *Scientific Reports*, *5*, 9879.

Lisignoli, G., Cristino, S., Piacentini, A., Toneguzzi, S., Grassi, F., Cavallo, C., … Facchini, A. (2005). Cellular and molecular events during chondrogenesis of human mesenchymal stromal cells grown in a three-dimensional hyaluronan based scaffold. *Biomaterials*, *26*, 5677–5686.

Makris, E. A., Gomoll, A. H., Malizos, K. N., Hu, J. C., & Athanasiou, K. A. (2015). Repair and tissue engineering techniques for articular cartilage. *Nature Reviews Rheumatology*, *11*, 21–34.

Marsich, E., Borgogna, M., Donati, I., Mozetic, P., Strand, B. L., Salvador, S. G., … Paoletti, S. (2008). Alginate/lactose-modified chitosan hydrogels: A bioactive biomaterial for chondrocyte encapsulation. *Journal of Biomedical Materials Research. Part A*, *84*, 364–376.

Martín, A., Patel, J. M., Zlotnick, H. M., Carey, J. L., & Mauck, R. L. (2019). Emerging therapies for cartilage regeneration in currently excluded 'red knee' populations. *Regenerative Medicine*, *4*, 12.

Montañez-Heredia, E., Irízar, S., Huertas, P. J., Otero, E., Del Valle, M., Prat, I., … Hernandez-Lamas, M. D. C. (2016). Intra-articular injections of platelet-rich plasma versus hyaluronic acid in the treatment of osteoarthritic knee pain: A randomized clinical trial in the context of the Spanish National Health Care System. *International Journal of Molecular Sciences*, *17*, 1064.

Mueller-Rath, R., Gavénis, K., Andereya, S., Mumme, T., Albrand, M., Stoffel, M., … Schneider, U. (2010). Condensed cellular seeded collagen gel as an improved biomaterial for tissue engineering of articular cartilage. *Bio-Medical Materials and Engineering*, *20*, 317–328.

Nava, M. M., Draghi, L., Giordano, C., & Pietrabissa, R. (2016). The effect of scaffold pore size in cartilage tissue engineering. *Journal of Applied Biomaterials & Functional Materials*, *14*, e223–e229.

Pan, J., Zhou, X., Li, W., Novotny, J. E., Doty, S. B., & Wang, L. (2009). In situ measurement of transport between subchondral bone and articular cartilage. *Journal of Orthopaedic Research*, *27*, 1347–1352.

Pang, H. T., Chen, X. G., Ji, Q. X., & Zhong, D. Y. (2008). Preparation and function of composite asymmetric chitosan/CM-chitosan membrane. *Journal of Materials Science. Materials in Medicine*, *19*, 1413–1417.

Poole, A. R., Kobayashi, M., Yasuda, T., Laverty, S., Mwale, F., Kojima, T., … Wu, W. (2002). Type II collagen degradation and its regulation in articular cartilage in osteoarthritis. *Annals of the Rheumatic Diseases*, *61* (Suppl. 2), ii78–ii81.

Ragetly, G. R., Slavik, G. J., Cunningham, B. T., Schaeffer, D. J., & Griffon, D. J. (2010). Cartilage tissue engineering on fibrous chitosan scaffolds produced by a replica molding technique. *Journal of Biomedical Materials Research*, *93A*, 46–55.

Rizwan, M., Yahya, R., Hassan, A., Yar, M., Abd Halim, A. A., Rageh Al-Maleki, A., … Zubairi, W. (2019). Novel chitosan derivative based composite scaffolds with enhanced angiogenesis; potential candidates for healing chronic non-healing wounds. *Journal of Materials Science. Materials in Medicine*, *30*, 72.

Salamanna, F., Giavaresi, G., Parrilli, A., Martini, L., Nicoli Aldini, N., Abatangelo, G., … Fini, M. (2019). Effects of intra-articular hyaluronic acid associated to Chitlac (arty-duo-®) in a rat knee osteoarthritis model. *Journal of Orthopaedic Research*, *37*, 867–876.

Sánchez-Téllez, D. A., Téllez-Jurado, L., & Rodríguez-Lorenzo, L. M. (2017). Hydrogels for cartilage regeneration, from polysaccharides to hybrids. *Polymers (Basel)*, *9*, 671.

Song, X., Zhu, C., Fan, D., Mi, Y., Li, X., Fu, R. Z., … Feng, R. R. (2017). A novel human-like collagen hydrogel scaffold with porous structure and sponge-like properties. *Polymers (Basel)*, *9*, 638.

Sophia Fox, A. J., Bedi, A., & Rodeo, S. A. (2009). The basic science of articular cartilage: Structure, composition, and function. *Sports Health*, *1*, 461–468.

Strauss, E., Schachter, A., Frenkel, S., & Rosen, J. (2009). The efficacy of intra-articular hyaluronan injection after the microfracture technique for the treatment of articular cartilage lesions. *The American Journal of Sports Medicine*, *37*, 720–726.

Toh, W. S., Lee, E. H., Guo, X. M., Chan, J. K. Y., Yeow, C. H., Choo, A. B., & Cao, T. (2010). Cartilage repair using hyaluronan hydrogel-encapsulated human embryonic stem cell-derived chondrogenic cells. *Biomaterials*, *31*, 6968–6980.

Wernecke, C., Braun, H. J., & Dragoo, J. L. (2015). The effect of intra-articular corticosteroids on articular cartilage: A systematic review. *Orthopaedic Journal of Sports Medicine*, *3*, 2325967115581163.

Yamane, S., Iwasaki, N., Majima, T., Funakoshi, T., Masuko, T., Harada, K., … Nishimura, S. (2005). Feasibility of chitosan-based hyaluronic acid hybrid biomaterial for a novel scaffold in cartilage tissue engineering. *Biomaterials*, *26*, 611–619.

How to cite this article: Scognamiglio F, Travan A, Borgogna M, Donati I, Marsich E. Development of biodegradable membranes for the delivery of a bioactive chitosan-derivative on cartilage defects: A preliminary investigation. *J Biomed Mater Res*. 2020;108:1534–1545. https://doi.org/10.1002/jbm.a.36924